The Cardiac Caval Index: Improving Noninvasive Assessment of Cardiac Preload

Original Article

The *cardiac caval index*. Improving non-invasive assessment of cardiac preload

Dr. Leonardo Ermini[1], Dr. Stefano Seddone[1], Dr. Piero Policastro[2], Prof. Luca Mesin[2], Dr. Paolo Pasquero[3], Prof. Silvestro Roatta[1]

[1] Laboratory of Integrative Physiology, Department of Neuroscience, Università di Torino, c.so Raffaello 30, 10125, Torino, Italy

[2] Mathematical Biology and Physiology, Department of Electronics and Telecommunications, Politecnico di Torino, c.so Duca degli Abruzzi 24, 10129, Torino, Italy

[3] Department of Medical Sciences, Università di Torino, c.so Achille Mario Dogliotti 14, 10126 Torino, Italy

ORCID:

LE: 0000-0002-3362-0623

SS: 0000-0002-1909-871X

PPo: 0000-0002-3154-7426

LM: 0000-0002-8239-2348

PPa: 0000-0002-5802-3446

SR: 0000-0001-7370-2271

Running title

The Cardiac Caval Index

Corresponding author: Leonardo Ermini, c.so Raffaello 30, 10125, Torino, Italy.

E-mail: leonardo.ermini@unito.it. Phone: +39 011 6708164.

Abstract

Objectives - Inferior Vena Cava (IVC) pulsatility quantified by the Caval Index (CI) is characterized by poor reliability, also due to the irregular magnitude of spontaneous respiratory activity generating the major pulsatile component. The aim of this study was to test whether the IVC cardiac oscillatory component could provide a more stable index (Cardiac CI - CCI) compared to CI or respiratory CI (RCI).

Methods - Nine healthy volunteers underwent long-term monitoring in supine position of IVC, followed by 3 min Passive Leg Raising (PLR). CI, RCI and CCI were extracted from video recordings by automated edge-tracking and CCI was averaged over each respiratory cycle (aCCI). Cardiac Output (CO), Mean Arterial Pressure (MAP) and Heart Rate (HR) were also recorded during baseline (1 min prior to PLR) and PLR (first minute).

Results - In response to PLR, all IVC indices decreased ($p<0.01$), CO increased by 4±4% ($p=0.055$) while HR and MAP did not vary. The Coefficient of Variation (CoV) of aCCI (13±5%) was lower than that of CI (17±5%, $p<0.01$), RCI (26±7%, $p<0.001$) and CCI (25±7%, $p<0.001$). The mutual correlations in time of the indices were 0.81 (CI-RCI), 0.49 (CI-aCCI) and 0.2 (RCI-aCCI).

Conclusions - Long-term IVC monitoring by automated edge-tracking allowed us to evidence that 1) respiratory and average cardiac pulsatility components are uncorrelated and thus carry different information and 2) the new index aCCI, exhibiting the lowest CoV while maintaining good sensitivity to blood volume changes, may overcome the poor reliability of CI and RCI.

Key Words: inferior vena cava; passive leg raising; volume status; fluid responsiveness; automatic edge tracking.

Introduction

In the clinical setting, deciding whether and what amount of fluid to administer intravenously to a patient, i.e., the prediction of fluid responsiveness, is a long-standing open issue, whose relevance is paramount. Indeed, it has been shown that only half of the haemodynamic unstable patients exhibits a positive outcome after a fluid challenge [1], while the remaining ones are exposed to the risk of fluid overload [2–4]. Since no satisfactory solution to this problem has been found yet, improvements in the existing techniques as well as new methodological approaches are constantly investigated [5–9].

Due to its fast and non-invasive approach, the echographic assessment of the Inferior Vena Cava (IVC) pulsatility is a widely adopted monitoring technique [7]. From the analysis of pulsatility, it possible to infer about the mechanical characteristics of blood vessels, such as stiffness and compliance, and about their determinants, such as blood pressure, blood volume, vessel tone, etc. (Mesin et al., *submitted*). IVC pulsatility is often quantified by means of the Caval Index (CI), which conveniently normalizes the respirophasic diameter variation (d_{max} - d_{min}) to d_{max}, thus accounting for individual differences in IVC size (d_{max} and d_{min} being the maximum and minimum diameters, as measured at the end of the expiratory and inspiratory phases, respectively). However, this index suffers of a large variability and, consequently, of poor reliability [10–12]. Based on the development of new image processing algorithms, several sources of variability were recently investigated and compensated for, e.g., by tracking the displacement of the vessel with respect to the ultrasound (US) probe [13,14] and by averaging the measurements over several IVC diameters in either short [15] or long axis [14,16], which contributed to improve the repeatability of the measurements [15,16]. However, a major source of variability in the respirophasic oscillation of IVC size is the intrinsic variability of spontaneous respiratory activity, in terms of magnitude, frequency and relative extent of thoracic/diaphragmatic

73 respiration [17,18], all these aspects providing consistent effects on IVC pulsatility [18–21]. A possible
74 solution to this problem was originally suggested by Nakamura [22] who proposed to consider
75 the cardiac component of IVC pulsatility rather than the respiratory. The issue was followed-
76 up in few subsequent studies [15,16,19,23]. In these studies, the automated analysis of US video
77 clips yielded the continuous description of IVC size changes with high time resolution (equal
78 to the frame rate of the US video recording), so that the cardiac and respiratory components of
79 IVC pulsatility could be easily separated, based on their different frequency contents, and
80 independently analysed [15,16,23]. On this basis, the respiratory CI (RCI) and the cardiac CI (CCI),
81 specifically quantifying the respiratory and cardiac component of IVC pulsatility, were
82 introduced and compared. The results showed that also the CCI could be used as an index of
83 vascular filling [22,23] and that it was characterized by a lower variability (as quantified by the
84 coefficient of variation, CoV) than the RCI, although, contrary to the expectation, not lower
85 than the variability of the CI [16]. Two reasons may possibly explain this observation: 1) the
86 above mentioned results refer to index variability over different subjects and measurement
87 sessions, while the actual CCI variability over time has never been assessed; 2) the cardiac
88 pulsatility may still be affected by a respiratory modulation, as apparent from published
89 recordings [16,24] and confirmed in preliminary observations. However, to our knowledge, all
90 studies generally considered only short time intervals lasting 10-15 s, and the time correlation
91 between pulsatile components has never been investigated.
92 We hypothesized that 1) by further improving the signal processing we could effectively
93 reduce the respiratory modulation of CCI and obtain a more stable hemodynamic index of
94 vascular filling; 2) due to its different nature, the CCI could differ from RCI and CI in terms of
95 time course and responsiveness to fluid challenges.

To this purpose, continuous and long-duration recordings of B-mode IVC imaging were performed with the help of a dedicated probe holder, in resting conditions and during a simulated fluid challenge, as produced by passive leg raising (PLR).

Materials and Methods

Subjects

Nine healthy volunteers (7 M, 2 F, age 34 ± 9) were included in the study, with the only exclusion criteria being a poor quality of the echographic imaging. The study was approved by the Ethics Committee of the University of Torino (March 23, 2015) and all participants gave their informed consent according to the principles of the Helsinki Declaration.

Experimental set-up and protocol

Participants remained supine on a clinical bed for at least 30 min before starting the experiment, in order to stabilize the equilibrium between fluid compartments [19,25]. A two-dimensional B-mode longitudinal view of the IVC was recorded by means of a MyLab 25 Gold system (ESAOTE, Genova, Italy) equipped with a convex 2-5 MHz US probe, according to a *subxiphoid* approach [26]. To achieve long-lasting ultrasound (US) monitoring, we made use of a probe holder, as successfully implemented in previous studies for stable echo-Doppler monitoring of arteries and veins of upper and lower limbs [9,27–30]. In the present case, the probe holder was stemming from one side of the bed and its 40-cm long horizontal arm was allowed to freely rotate about a joint at one of its ends. The US probe, located at the other end, due to its own weight, could then exert a light pressure on the abdomen and maintain adequate acoustic contact, accommodating with virtually vertical displacements the small abdominal

movements during respiration. This arrangement allowed us to continuously monitor the IVC for the whole duration of the protocol (4 min).

The experimental protocol consisted of 1 min of rest in supine position (baseline), followed by 3 min during which the legs were passively raised and maintained at about 45 deg (passive leg raising, PLR) and 1 min of rest, again in supine position. During the entire protocol, the US video of the IVC longitudinal section (in the sagittal plane) was recorded for the subsequent processing and analysis. In addition, Heart Rate (HR), Mean Arterial Pressure (MAP) and Cardiac Output (CO) were non-invasively monitored by photoplethysmography (CNAP®, CNSystems Medizintechnik, Graz, Austria) while breathing was monitored by means of a custom-made strain gauge band placed around the chest (the recorded signal is referred to as Breath in the following). All these signals were digitally and synchronously recorded by a general-purpose acquisition board (Micro 1401 IImk, CED, Cambridge, UK, with Spike2 software): IVC videos were acquired at about 30 fps while HR, MAP, CO and breathing were sampled at 10 Hz.

IVC segmentation

US videos were processed by a custom-made software (implemented in MATLAB 2020a, The MathWorks, Natick, MA) for IVC edge-tracking. The routines were based on a previously developed algorithm [14]. The tracking algorithm was improved to attenuate the effect of small drifts, which would produce detrimental effects with videos of long duration considered here (manuscript in preparation). The edges of the IVC were estimated as previously described [14], by sampling along 21 directions crossing the blood vessel, considering a portion selected by an operator (PPo), who was blinded to the results. Along each direction, the software estimated the US pixel intensity by interpolation. Then, abrupt variations of this estimated US intensity were identified as the locations of the two IVC edges along the considered direction (see Mesin

et al. [14] for additional details). The length of the segment between each couple of points placed on the upper and lower vein edges was the IVC diameter along that direction.

The median axis of the vein was estimated (as the mean of the two sampled edges), interpolated by a second order polynomial and used to rotate the 21 diameters mentioned above to be orthogonal to it. By considering all frames of the US video, each diameter was a time series. High frequency contributions in these time series of diameters (mostly related to superimposed noise) were removed. For the identification of the cut-off frequency, the power spectrum density (PSD) of the diameters was first computed (Burg method, with order 40 [31]), from which the highest frequency of our interest was identified as follows. First, we have searched for a peak in the PSD between 40bpm and 120bpm, which reflected the cardiac component. Then, the median (across diameters) of peak frequencies (mf) was computed (this parameter was used later to define the cut-off frequency of the filter). Then, a portion of 15 mm around the position of the diameter showing the highest peak of the cardiac component was selected (assuming that such a diameter provided reliable information on the cardiac contribution and that it was less affected by noise than the other diameters). Upper and lower border points of this portion of the vein were then interpolated with two straight lines. Finally, the *mean IVC diameter*, for each frame, was calculated as the area of the IVC section considered above, divided by its length (i.e., 15 mm).

Such a mean diameter was low pass filtered, with cut-off frequency equal to $mf + 0.5Hz$ (Chebyshev of type I, stop band starting at $mf + 1.5Hz$, minimum attenuation of 30 dB, passband from 0 to $mf + 0.5Hz$ with ripple of 0.5 dB) and indicated with *dIVC*.

The respiratory and cardiac components of IVC pulsatility were estimated from the mean diameter just obtained. The respiratory diameter, indicated as *R-dIVC,* was estimated by the first step of the Empirical Mode Decomposition applied to the mean diameter. Specifically, two curves were first obtained by interpolating the local maxima and the local minima of *dIVC*.

166 The curve *R-IVC* was defined as the mean of these two curves. Notice that this technique allows
167 to estimate each respiration cycle. On the other hand, a filter with fixed passband was used in
168 previous works [16]: such a filter had lower performances than the one used here, especially with
169 our long recordings, in which respiration cycles could have very different durations (thus, being
170 attenuated differently by a fixed filter). The cardiac diameter, called C-dIVC, was computed as
171 $C\text{-}dIVC = dIVC - R\text{-}dIVC + s\text{-}dIVC$ and is equivalent to the mean diameter deprived of the
172 respiratory oscillations. The term *s-dIVC* indicates the lowpass filtered mean diameter with cut-
173 off 0.05 Hz (Chebyshev filter of type I, stop band starting at 0.5 Hz, minimum attenuation of
174 30 dB, passband ripple of 0.5 dB), where only the *slow* sub respiratory frequencies are left.
175 This low pass filter was chosen in order to remove any oscillation and keep only the low
176 frequency trend reflecting slow IVC size variations induced by the PLR.
177 At this point of the analysis, the three diameters, *dIVC*, *R-dIVC* and *C-dIVC* were available
178 as time series (see Fig. 1) and were used to estimate the collapsibility indicators Caval Index
179 (CI), Respiratory Caval Index (RCI) and Cardiac Caval Index (CCI) respectively, according to
180 the usual formula: $(d_{max} - d_{min})/d_{max}$ (Fig. 1, bottom). Note that, while for CI and RCI one
181 estimate per respiratory cycle is obtained, the CCI yields one estimate per cardiac cycle.
182 In addition, an *averaged* version of the CCI, aCCI, was computed by averaging the CCI
183 over distinct respiratory cycles. The aCCI estimates could then be considered synchronous with
184 CI and RCI (one estimate per respiratory cycle).

185 *Data analysis*

186 HR, MAP and CO were exported from Spike2 software to MATLAB® (version 2020b) for
187 off-line analysis. As a first step, they were aligned in time with the time-series of the IVC
188 collapsibility indexes, computed separately as explained above, that presented a non-uniform
189 sampling rate due to their nature. Indeed, CI, RCI and aCCI had one sample per respiratory

190 cycle while CCI one per heartbeat: the sample location in time, within the respiratory cycle,
191 was arbitrary and we chose to be at the minimum of the IVC diameter component for all the
192 three indexes.

193 The intra-subject variability in time of each IVC collapsibility index was quantified during
194 baseline by the coefficient of variation (CoV = (STD / MEAN) × 100) and averaged across all
195 subjects. The correlation of time course in baseline was tested among CI, RCI and aCCI, for
196 each subject, using the Pearson correlation coefficient (ρ); then, the mean ρ across subjects was
197 computed by averaging the individual ρ values after a Fisher Z-transformation and
198 subsequently applying an inverse transformation to the result.

199 In order to perform the correlation of IVC indices with other signals, they were resampled
200 at 10 Hz, after a shape-preserving piecewise cubic interpolation. This was necessary to test the
201 correlation of CCI and aCCI with the respiratory pattern. However, since the delay between
202 the respiratory effort and the resulting changes in size of the IVC cannot be assumed constant
203 neither across subject nor over time, the normalized cross-correlation function on the
204 appropriately standardized signals, instead of Pearson correlation coefficient, was employed
205 and its maximum value, irrespective of the delay, was chosen as the correlation coefficient (ρ).
206 Then, the ρ values obtained were averaged across subjects using the Fisher transformation as
207 explained above.

208 The response to the PLR is known to take place within the first minute after raising the legs
209 [32] and, for each of the variables, it was assessed as the difference between the mean value
210 calculated during the first minute of PLR and during the whole baseline (1 min), as DELTA =
211 PLR - baseline, and considered in both absolute and relative (percentage) terms. For both basal
212 and DELTA values, mutual correlations among CI, RCI and aCCI were quantified by the
213 Pearson correlation coefficient, presented along with the 95% confidence interval in between
214 brackets. The effect of PLR on each variable was assessed considering the distribution of

DELTA values and testing if the mean differed from zero with a level of significance set at 0.05, by means of the Wilcoxon signed rank test. The same test was used to compare the variability in time (as expressed by the CoV) of aCCI with CI and RCI. The IVC indices accuracy in predicting the subject response to the simulated fluid challenge, as induced by PLR, was analysed by means of Receiver Operating Characteristic (ROC) curves built using a 10% increase in CO as marker of fluid responsiveness [6,33].

Finally, it is worth to mention that, given the non-uniform sampling rate for the IVC collapsibility indexes, their average time course, across subjects, was obtained by averaging the interpolated curves.

Results

Basal conditions

An example of the original tracings from a representative subject is shown in Figure 1 which includes the continuous recordings of some systemic variables like HR, MAP, and respiratory activity as well as variables extracted from the US monitoring of the IVC, i.e., the IVC diameter (average diameter of the considered IVC segment), the respiratory diameter (high frequency components are filtered out) and the cardiac diameter (the respiratory component is filtered out). At the bottom of the figure are the different indices, automatically calculated. Two aspects need to be observed.

1) A strong correspondence exists between the magnitude of respiratory acts and the respiratory changes in IVC diameter. Accordingly, CI and RCI (bottom) are also modulated by the depth of respiration, in particular, it is worth to notice how CI and RCI drop (the variation is in the order of 10%) around the fourth second of the

recording, concomitantly with a reduced inspiratory depth, as revealed by the Breath signal.

2) Even the cardiac pulsatility is modulated by the respiratory activity. Accordingly, such modulation is preserved in CCI and affects its variability in time.

We first tested whether the averaging over single respiratory cycles, as implemented for the calculation of aCCI, was effective in reducing the respiratory modulation affecting CCI. In Figure 2, the distributions of the maxima of the cross-correlation in time between Breath and the two indexes, CCI and aCCI, are shown. Note that the averaging introduced in aCCI has drastically reduced the correlation with respiration from 0.4 (for CCI) to 0.02 (for aCCI).

We then tested whether this new feature was effective in reducing the overall variability in time, as assessed by the CoV. In Figure 3 it is possible to observe the distribution of the individual CoVs, depicted by means of box and whiskers plots, for each IVC collapsibility index, including the original CCI. The MEAN ± STD CoV values of CI, RCI, CCI and aCCI are, respectively, 17 ± 5 %, 26 ± 7 %, 25 ± 7 %, 13 ± 5 %. As expected, aCCI exhibited a lower variability than CCI. The improved stability over time can also be observed by comparing the corresponding tracings in Figure 1. Moreover, aCCI also achieved a lower CoV than CI ($p<0.01$).

Response to PLR

On a different timescale, the full representation of the response to PLR is shown in Figure 4. It can be observed that during PLR, starting at time 0 s, both cardiac and respiratory pulsatile components are reduced, and that the IVC diameter is increased. This results in a reduction of all indices during PLR, as displayed at the bottom.

In Figure 5, the averaged (across subjects) time course of HR, MAP and CO are presented in terms of percentage changes with respect to the mean baseline value (i.e., DELTA in

261 percentage terms). It can be observed that at the beginning of PLR (time 0 s), HR and MAP
262 exhibit only small fluctuations while CO immediately begins to rise reaching a peak at around
263 30 s and returning to the basal value at around 60 s, before the end of PLR (180 s).

264 Figure 6 shows, on the same timescale, the time course of IVC collapsibility indexes,
265 namely CI, RCI and aCCI (with CCI superimposed as dashed line). Here the variations with
266 respect to the mean baseline values are not translated in percentage terms, since the indexes are
267 already expressed as percentages, so that absolute variations (of a percentage) are considered
268 (i.e., DELTA in absolute terms). It can be observed that all indices exhibit a consistent decrease,
269 which is maintained througout PLR, and that aCCI exhibited a sharper decrease at the
270 beginning of PLR, compared to CI and RCI.

271 In Table 1, the values averaged across subjects for baseline, PLR, and DELTA (in
272 percentage terms) for all the physiological variables of interest are listed, as well as the
273 statistical significance against the null hypothesis of no effects induced by PLR. As it can be
274 noticed, HR and MAP did not change following PLR while CO and all the IVC collapsibility
275 indexes did.

276 Finally, regarding the prediction of fluid responsiveness, both CI and aCCI performed as
277 perfect classifiers (i.e., AUCROC 1) with threshold of 21% and 9%, respectively, while RCI
278 reached a poorer performance (AUCROC 0.78).

279 *Correlations among indices*

280 In Figure 7, the distributions of the individual mutual correlations in time among the IVC
281 collapsibility indexes are shown (the original CCI is no longer considered): the biggest
282 correlation is between CI and RCI (mean value 0.81), while the smallest one is between RCI
283 and aCCI (mean value 0.2). It is worth to notice how the small interquartile range of CI-RCI
284 distribution, depicted in Figure 7, highlights the robustness of the link between the two indexes,

while the same cannot be asserted for the CI-aCCI correlation in time, despite the relatively high mean value (0.49). Finally, the Pearson correlation coefficient among the averaged baseline values of CI-RCI, CI-aCCI and RCI-aCCI was 0.92 (0.66, 0.98), 0.76 (0.19, 0.95) and 0.50 (-0.25, 0.87), respectively. The same coefficients for the DELTA values, following the same order, were 0.74 (0.16, 0.94), 0.73 (0.13, 0.94), 0.2 (-0.53, 0.76).

Discussion

The present study allowed to confirm preliminary observations and to achieve new relevant results, which can be synthetized as follows:

1) Although the CI is generally considered as an index of the respiratory-induced pulsatility of the IVC, it is heavily affected (or disturbed) by a pulsatility of cardiac nature.
2) The magnitude of the cardiac pulsatility of IVC is still modulated by the respiratory activity, which negatively impacts on the reliability of the CCI.
3) Averaging the CCI over single respiratory cycles effectively eliminates the respiratory modulation and improves its stability in time.
4) The averaged cardiac collapsibility index (aCCI) responsiveness to PLR is uncorrelated to the respiratory collapsibility index (RCI), suggesting that the two indices may carry different information.

To our knowledge, this is the first study reporting a long-term monitoring and analysis of IVC pulsatility, which was achieved thanks to a newly devised experimental set-up and consolidated image processing algorithms [13,14,16,24,34]. With this approach, a continuous time series of the average IVC diameter, with high time resolution, could be analysed along with other physiological variables: such an analysis included the identification of the oscillatory

components of the IVC diameter of respiratory and cardiac origin and the automated calculation of the corresponding collapsibility indices RCI and CCI (Fig. 1) [16].

The pivotal role of heart in Inferior Vena Cava respirophasic oscillations

The aforementioned framework gave us the possibility to carefully observe the interplay between respiration and heartbeat in generating the IVC pulsatility. Indeed, although IVC pulsatility has been already the object of hundreds of studies [11,12] and its use in the clinical settings, as predictor of fluid responsiveness [6,7] or as surrogate measure of central venous pressure [34], has been extensively investigated, only recently the cardiac component of the IVC pulsatility has been described [22]. This component was probably too weak or too fast to be detected and disentangled from the slower respiratory component by means of just the visual assessment and the standard tools available on US machines. On the one hand, these limitations delayed the recognition and the investigation of the characteristics and meaning of the cardiac component, on the other hand, the unrecognized cardiac oscillation, merging with the primary respiratory oscillation, decreased the "signal-to-noise ratio" and increased the variability of the oscillatory pattern. We speculate that this overlooked "disturbance" on the assessment of IVC diameter may at least partly explain the poor reliability and clinical applicability of the CI [11,12]. Notably, in the present study, removal of the cardiac pulsatility reduced the IVC collapsibility index by about 50% (i.e., RCI is about 50% of CI) and, accordingly, the aCCI approximately accounts for the other 50% (see Table 1, baseline). These results challenge the concept that the classical IVC CI quantifies the "respirophasic" changes in IVC diameter.

As shown in the representative recordings of Figure 1, as well as in other figures previously published [15,16], the cardiac pulsatility is modulated by respiration: the magnitude of the oscillation increases at low IVC diameter, which occurs approximately at the end of the inspiratory phase (maximum lung volume). This modulatory pattern fits with the idea that the

pulse pressure, mainly provided by the atrial contraction, results in a lower volume increase (reflected by a lower IVC diameter increase) when the IVC compliance is lower, which occurs at larger IVC size (Mesin et al, *submitted*). Surprisingly an opposite pattern is shown in Figure 4 of the study from Sonoo et al [23], i.e., wider cardiac pulsatility during expiration compared to inspiration. However, their average findings (collected from 142 patients enrolled in an emergency department) confirms a higher CCI during inspiration (13.8%) compared to expiration (11.0%). This modulatory action is responsible for the high CoV of the CCI in time, similar to the CoV of CI (Fig. 3) [16] and negatively impacts on its potential clinical usefulness. By simply averaging over single respiratory cycles (aCCI), this problem was effectively addressed and the CoV in time considerably reduced.

As discussed above, cardiac pulsatility is larger when the vessel size is smaller and vessel compliance is larger. As such, aCCI candidates as a possible indicator of IVC compliance and of poor vascular filling. In this respect, it is interesting to observe that it was shown to correlate to CI, both in time (intra-subject) and across different subjects (in basal conditions). Moreover, it was significantly affected by PLR (-28%, $p<0.01$).

On the other hand, while a similar performance was reported by RCI (good correlation with CI and significant decrease during PLR), aCCI and RCI were very poorly correlated: their spontaneous oscillations in resting conditions are uncorrelated, their absolute values assessed in resting conditions are uncorrelated, their responses to a (simulated) fluid challenge are uncorrelated. These results strongly suggest that RCI and CCI are carrier of different information (although both sensitive to fluid challenges). Their different time course in the response to PLR (Fig. 6, aCCI exhibiting a faster and sharper response than RCI) further supports this proposition.

Clinical implications

While further studies are necessary to understand the distinct physio-pathological meaning of the two indices and their possible integration for clinical purposes, the possibility to get increased and more reliable information from the same fast and non-invasive US examination is intriguing. To date, only few studies have included a cardiac IVC collapsibility index in their outcomes. In particular, the presence of CCI enhanced the capacity to predict the volume status [24] and right atrial pressure in patients [34] . However, no one has yet investigated the potential of CCI in predicting a fluid challenge. For this reason, although we were curious to perform such an investigation, we are aware that, given our small dataset (N=9) and the limitations of the photoplethysmographic finger-cuff pulse contour analysis techniques in reliably monitoring CO [35], the extrapolated ROC analysis presented in this work are not relevant for a valid fluid responsiveness study. Beyond that, we believe that the present findings, although obtained on healthy volunteers, can add new useful information to the widespread use of the IVC collapsibility indexes in predicting the fluid responsiveness in patients. Finally, the possibility that CCI could be influenced by additional factors related to pathological alterations of cardiac function, e.g., contractility, stiffness, valvular efficiency, etc., as well as changes in intra-abdominal pressure, remains to be explored and deserves further studies on specific patient populations.

Physiologic response to Passive Leg Raising

A final comment concerns the general response to PLR in this group of healthy subjects, which provides a nice description of the physiological adaptation of the body to the new situation (Figs. 5 and 6): no apparent effect on MAP, only a minor (pre-) activation of HR, probably an increase in alertness due to the passive leg movement, along with a small but visible transient increase in CO [32]. In comparison, all the IVC indices detect a net variation

during PLR. Interestingly the exhibited changes are not transient, but last throughout the 3-min duration of the test, which likely indicates that this time is too short for adjustments in blood volume. Moreover, they show that the duration of the transients is shorter at the onset (< 15 s) than at the termination of PLR (about 1 min).

Limitations

One limitation of the study is related to the way IVC videos were acquired, i.e., with the probe held in place by a probe holder rather than by the hand of the echographer. While this was a necessary implementation to achieve stable recordings lasting several minutes, it is not without drawbacks, as involuntary spontaneous movements of the subject as well as movements resulting from the PLR manoeuvre could occasionally interrupt the correct IVC tracking. However, thanks to the prompt intervention of the operators, the proper probe orientation was generally restored within seconds with no impact on the subsequent analysis. Prospectively, with the increasing adoption of 4D US machines, the edge-tracking will be likely extended to 3D images, which will minimize misalignment problems related to latero-lateral displacement of IVC with respect to both hand-held and fixed US probe.

Secondly, the experiment was performed only on healthy volunteers posing some limitations to the extrapolation of the results to the clinical setting. Moreover, we had to exclude subjects that could not present good quality imaging of the IVC, as required by the image processing routines. This criterion slightly biased the recruited sample towards a prevalence of males, possibly due to their lower thickness of abdominal adipose tissue layer. However, we are not aware of sex-related differences in IVC indices that could have affected the general validity of the present results. Unfortunately, this is a known limitation of US studies that require high quality imaging.

Conclusions

With this methodological study on healthy subjects, we evidenced that through echographic long-term monitoring of the IVC longitudinal section, in association with an automated edge tracking software, it is possible to record the IVC diameter and distinct respiratory and cardiac collapsibility indexes as continuous time-series. A newly defined *averaged cardiac collapsibility index*, aCCI, exhibited 1) the lowest variability in time, 2) good sensitivity to simulated blood volume changes, as induced by PLR and 3) poor correlation with the RCI in time, among subjects, and in their response to PLR, supporting the hypothesis that they carry different information. Therefore, we believe that aCCI has the potential to overcome the poor reliability of the classical CI in the fluid responsiveness prediction. Further studies in patients are needed to understand its specificity and explore its applicability in the clinical practice.

Funding Information

This activity was supported by local grants (ROAS_RILO_17_01), University of Torino, and by Proof of Concept "Vein Image Processing for Edge Rendering – VIPER", supported by the Italian Ministry of Economic Development, CUP C16I20000080006.

Conflict of Interest

An instrument implementing the algorithm used in this report to automatically track IVC edges and to extract the mean IVC diameter was patented by Politecnico of Torino and University of Torino (WO 2018/134726).

References

1. Bentzer P, Griesdale DE, Boyd J, MacLean K, Sirounis D, Ayas NT. Will This Hemodynamically Unstable Patient Respond to a Bolus of Intravenous Fluids? *JAMA*. 2016;316(12):1298-1309. doi:10.1001/JAMA.2016.12310
2. Sakr Y, Rubatto Birri PN, Kotfis K, et al. Higher Fluid Balance Increases the Risk of Death from Sepsis: Results from a Large International Audit∗. *Crit Care Med*. 2017;45(3):386-394. doi:10.1097/CCM.0000000000002189
3. Malbrain MLNG, Van Regenmortel N, Saugel B, et al. Principles of fluid management and stewardship in septic shock: it is time to consider the four D's and the four phases of fluid therapy. *Ann Intensive Care*. 2018;8(1):66. doi:10.1186/s13613-018-0402-x
4. Silva JM, de Oliveira AMR, Nogueira FAM, et al. The effect of excess fluid balance on the mortality rate of surgical patients: a multicenter prospective study. *Crit Care*. 2013;17(6):R288. doi:10.1186/cc13151
5. Monnet X, Marik PE, Teboul J-L. Prediction of fluid responsiveness: an update. *Ann Intensive Care*. 2016;6(1):1-11. doi:10.1186/S13613-016-0216-7
6. Monnet X, Teboul JL. Assessment of fluid responsiveness: Recent advances. *Curr Opin Crit Care*. 2018;24(3):190-195. doi:10.1097/MCC.0000000000000501
7. Shi R, Monnet X, Teboul JL. Parameters of fluid responsiveness. *Curr Opin Crit Care*. 2020;26(3):319-326. doi:10.1097/MCC.0000000000000723
8. Bednarczyk JM, Fridfinnson JA, Kumar A, et al. Incorporating Dynamic Assessment of Fluid Responsiveness Into Goal-Directed Therapy: A Systematic Review and Meta-Analysis. *Crit Care Med*. 2017;45(9):1538-1545. doi:10.1097/CCM.0000000000002554
9. Ermini L, Chiarello NE, De Benedictis C, Ferraresi C, Roatta S. Venous Pulse Wave Velocity variation in response to a simulated fluid challenge in healthy subjects.

Biomed Signal Process Control. 2021;63(102177). doi:10.1016/j.bspc.2020.102177

10. Long E, Oakley E, Duke T, Babl FE. Does Respiratory Variation in Inferior Vena Cava Diameter Predict Fluid Responsiveness: A Systematic Review and Meta-Analysis. *Shock*. 2017;47(5):550-559. doi:10.1097/SHK.0000000000000801

11. Das SK, Choupoo NS, Pradhan D, Saikia P, Monnet X. Diagnostic accuracy of inferior vena caval respiratory variation in detecting fluid unresponsiveness: a systematic review and meta-analysis. *Eur J Anaesthesiol*. 2018;35(11):831-839. doi:10.1097/EJA.0000000000000841

12. Orso D, Paoli I, Piani T, Cilenti FL, Cristiani L, Guglielmo N. Accuracy of Ultrasonographic Measurements of Inferior Vena Cava to Determine Fluid Responsiveness: A Systematic Review and Meta-Analysis. *J Intensive Care Med*. 2020;35(4):354-363. doi:10.1177/0885066617752308

13. Mesin L, Pasquero P, Albani S, Porta M, Roatta S. Semi-automated Tracking and Continuous Monitoring of Inferior Vena Cava Diameter in Simulated and Experimental Ultrasound Imaging. *Ultrasound Med Biol*. 2015;41(3):845-857. doi:10.1016/J.ULTRASMEDBIO.2014.09.031

14. Mesin L, Pasquero P, Roatta S. Tracking and Monitoring Pulsatility of a Portion of Inferior Vena Cava from Ultrasound Imaging in Long Axis. *Ultrasound Med Biol*. 2019;45(5):1338-1343. doi:10.1016/J.ULTRASMEDBIO.2018.10.024

15. Mesin L, Pasquero P, Roatta S. Multi-directional Assessment of Respiratory and Cardiac Pulsatility of the Inferior Vena Cava From Ultrasound Imaging in Short Axis. *Ultrasound Med Biol*. 2020;46(12):3475-3482. doi:10.1016/J.ULTRASMEDBIO.2020.08.027

16. Mesin L, Giovinazzo T, D'Alessandro S, et al. Improved Repeatability of the Estimation of Pulsatility of Inferior Vena Cava. *Ultrasound Med Biol*.

2019;45(10):2830-2843. doi:10.1016/J.ULTRASMEDBIO.2019.06.002

17. Tobin MJ, Mador MJ, Guenther SM, Lodato RF, Sackner MA. Variability of resting respiratory drive and timing in healthy subjects. *J Appl Physiol*. 1988;65(1):309-317. doi:10.1152/JAPPL.1988.65.1.309

18. Gignon L, Roger C, Bastide S, et al. Influence of Diaphragmatic Motion on Inferior Vena Cava Diameter Respiratory Variations in Healthy Volunteers. *Anesthesiology*. 2016;124(6):1338-1346. doi:10.1097/ALN.0000000000001096

19. Folino A, Benzo M, Pasquero P, et al. Vena Cava Responsiveness to Controlled Isovolumetric Respiratory Efforts. *J Ultrasound Med*. 2017;36(10):2113-2123. doi:10.1002/JUM.14235

20. Kimura BJ, Dalugdugan R, Gilcrease III GW, Phan JN, Showalter BK, Wolfson T. The effect of breathing manner on inferior vena caval diameter†. *Eur J Echocardiogr*. 2011;12(2):120-123. doi:10.1093/ejechocard/jeq157

21. Bortolotti P, Colling D, Colas V, et al. Respiratory changes of the inferior vena cava diameter predict fluid responsiveness in spontaneously breathing patients with cardiac arrhythmias. *Ann Intensive Care*. 2018;8(1):79. doi:10.1186/s13613-018-0427-1

22. Nakamura K, Tomida M, Ando T, et al. Cardiac variation of inferior vena cava: new concept in the evaluation of intravascular blood volume. *J Med Ultrason*. 2013;40(3):205-209. doi:10.1007/S10396-013-0435-6

23. Sonoo T, Nakamura K, Ando T, et al. Prospective analysis of cardiac collapsibility of inferior vena cava using ultrasonography. *J Crit Care*. 2015;30(5):945-948. doi:10.1016/J.JCRC.2015.04.124

24. Mesin L, Roatta S, Pasquero P, Porta M. Automated volume status assessment using Inferior Vena Cava pulsatility. *Electronics*. 2020;9(10):1671. doi:https://doi.org/10.3390/electronics9101671

25. Hagan RD, Diaz FJ, Horvath SM. Plasma volume changes with movement to supine and standing positions. *J Appl Physiol*. 1978;45(3):414-418. doi:10.1152/JAPPL.1978.45.3.414

26. Finnerty NM, Panchal AR, Boulger C, et al. Inferior Vena Cava Measurement with Ultrasound: What Is the Best View and Best Mode? *West J Emerg Med*. 2017;18(3):496. doi:10.5811/WESTJEM.2016.12.32489

27. Messere A, Ceravolo G, Franco W, Maffiodo D, Ferraresi C, Roatta S. Increased tissue oxygenation explains the attenuation of hyperemia upon repetitive pneumatic compression of the lower leg. *J Appl Physiol*. 2017;123(6):1451-1460. doi:10.1152/japplphysiol.00511.2017

28. Messere A, Turturici M, Millo G, Roatta S. Repetitive muscle compression reduces vascular mechano-sensitivity and the hyperemic response to muscle contraction. *J Physiol Pharmacol*. 2017;68(3):427-437.

29. Messere A, Tschakovsky M, Seddone S, et al. Hyper-Oxygenation Attenuates the Rapid Vasodilatory Response to Muscle Contraction and Compression. *Front Physiol*. 2018;9:1078.

30. Ermini L, Ferraresi C, De Benedictis C, Roatta S. Objective Assessment of Venous Pulse Wave Velocity in Healthy Humans. *Ultrasound Med Biol*. 2020;46(3):849-854. doi:10.1016/j.ultrasmedbio.2019.11.003

31. Kay SM. *Modern Spectral Estimation: Theory and Application*. Pearson Education India; 1988.

32. Monnet X, Teboul J-L. Passive leg raising: five rules, not a drop of fluid! *Crit Care*. 2015;19(1):18. doi:10.1186/s13054-014-0708-5

33. Mesquida J, Gruartmoner G, Ferrer R. Passive leg raising for assessment of volume responsiveness: A review. *Curr Opin Crit Care*. 2017;23(3):237-243.

doi:10.1097/MCC.0000000000000404

34. Albani S, Pinamonti B, Giovinazzo T, et al. Accuracy of right atrial pressure estimation using a multi-parameter approach derived from inferior vena cava semi-automated edge-tracking echocardiography: a pilot study in patients with cardiovascular disorders. *Int J Cardiovasc Imaging*. 2020;36(7):1213-1225. doi:10.1007/s10554-020-01814-8

35. Saugel B, Hoppe P, Nicklas JY, et al. Continuous noninvasive pulse wave analysis using finger cuff technologies for arterial blood pressure and cardiac output monitoring in perioperative and intensive care medicine: a systematic review and meta-analysis. *Br J Anaesth*. 2020;125(1):25-37. doi:https://doi.org/10.1016/j.bja.2020.03.013

Figures with captions

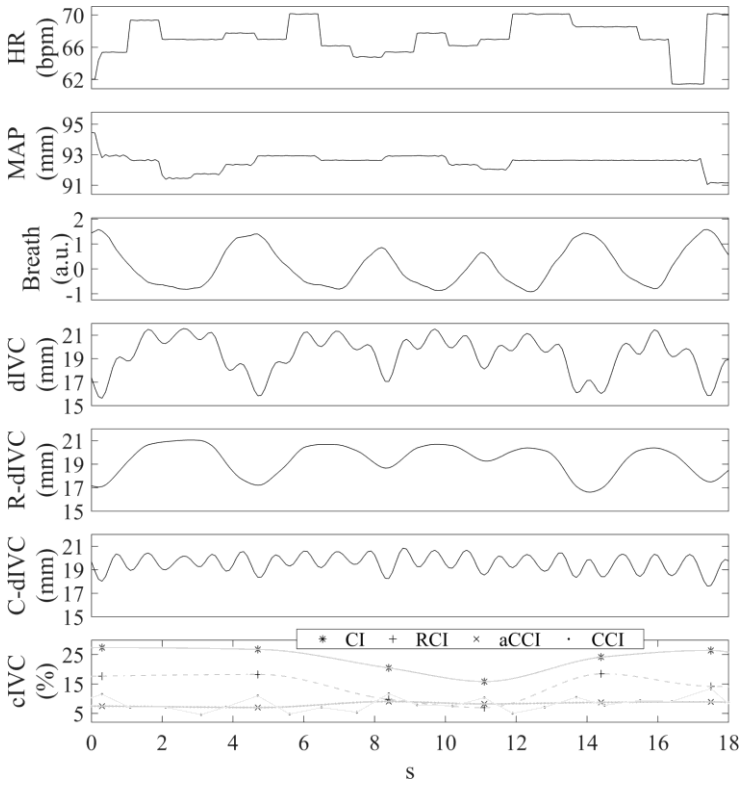

Fig. 1. Tracings from a representative subject, in resting condition. The time course of each one of the following variables is shown: Heart Rate (HR), Mean Arterial Pressure (MAP), Respiration (Breath), Inferior Vena Cava (IVC) respiratory (R-dIVC) and cardiac (C-dIVC) components of the native diameter trace (dIVC) and their respective indexes, namely Caval Index (CI), Respiratory Caval Index (RCI) and averaged Cardiac Caval Index (aCCI). In the latter graph, the markers indicate the exact sample of each IVC collapsibility indexes, as described in the legend, while the continuous grey lines are the respective cubic interpolation that were superimposed for a better visualization.

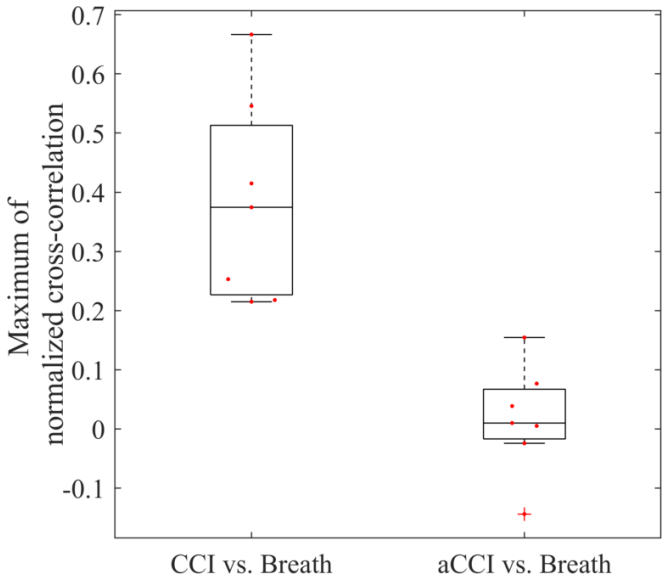

Fig. 2. Correlation between respiration and inferior vena cava (IVC) cardiac collapsibility indexes. Distribution of the individual maximum value of cross-correlation among breathing signal and the two versions of the cardiac IVC collapsibility index (native and averaged, CCI and aCCI, respectively), during baseline.

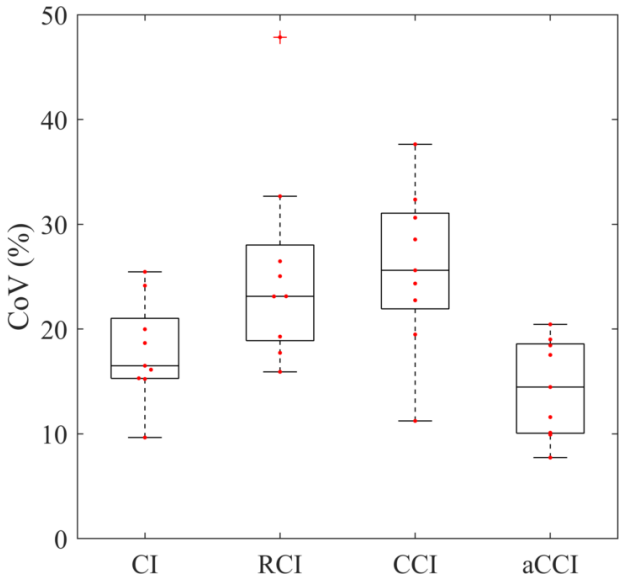

Fig. 3. Coefficient of Variation (CoV) of collapsibility indexes of the inferior vena cava. The CoV distributions across subjects computed during baseline are shown for Caval Index (CI), Respiratory Caval Index (RCI), Cardiac Caval Index (CCI) and averaged Cardiac Caval Index (aCCI). The red dots indicate the individual data.

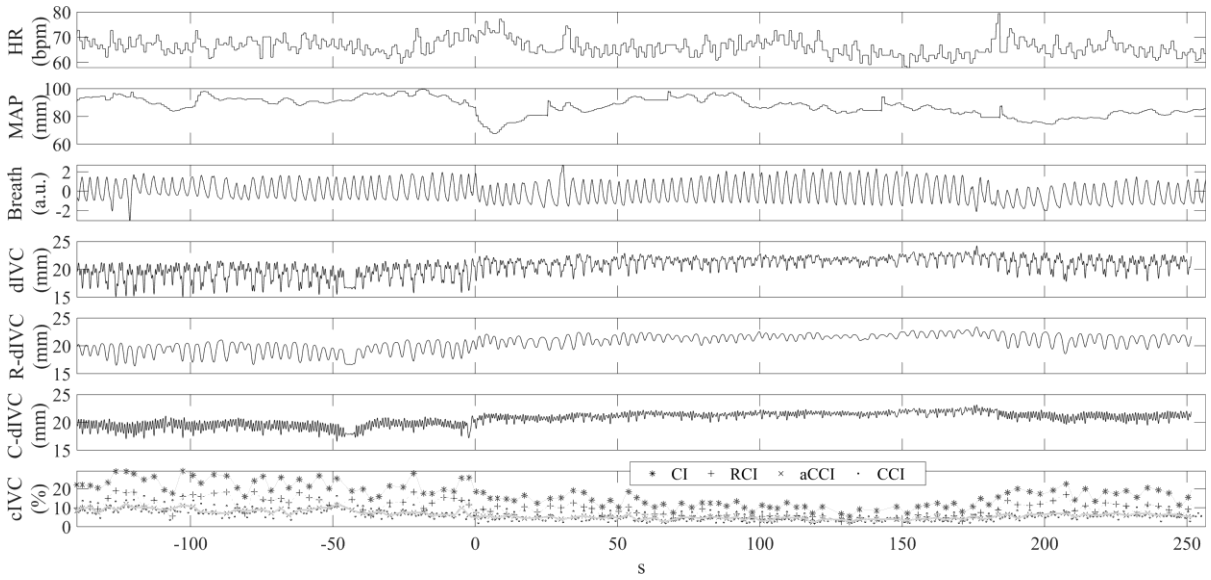

Fig. 4. Example of a complete individual recording. The time course of each one of the following variables is shown: Heart Rate (HR), Mean Arterial Pressure (MAP), Respiration (Breath), Inferior Vena Cava (IVC) respiratory (R-dIVC) and cardiac (C-dIVC) components of the native diameter trace (dIVC) and their respective indexes, namely Caval Index (CI), Respiratory Caval Index (RCI) and averaged Cardiac Caval Index (aCCI). In the latter graph, the markers indicate the exact sample of each IVC collapsibility indexes, as described in the legend, while the continuous grey lines are the respective cubic interpolation that were superimposed for a better visualization.

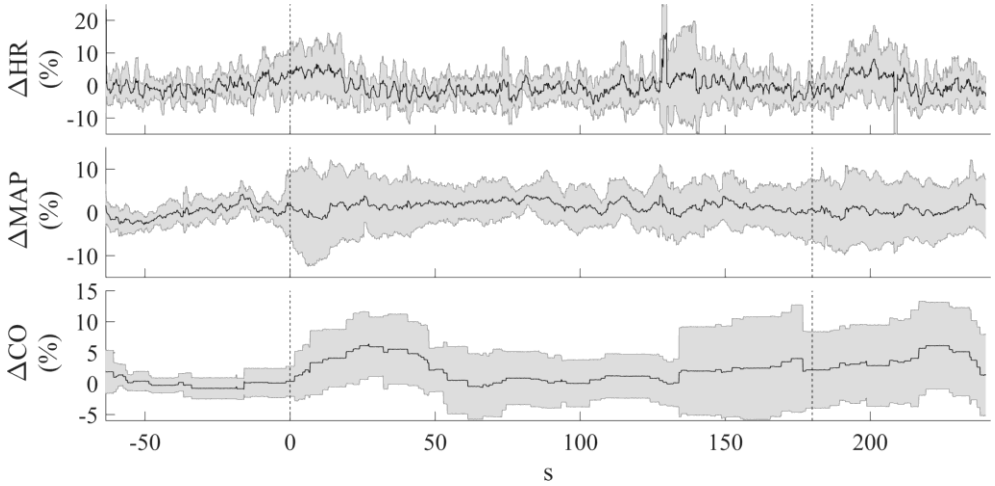

568

569 **Fig. 5.** Haemodynamic variables averaged (across subjects) time course. Percentage changes
570 with respect to the mean baseline value of Heart Rate (ΔHR), Mean Arterial Pressure (ΔMAP)
571 and Cardiac Output (ΔCO): the black solid line represents the mean while the shaded grey error
572 bar represent mean ± std. The vertical dashed lines mark the beginning (left one) and the end
573 (right one) of the PLR.

574

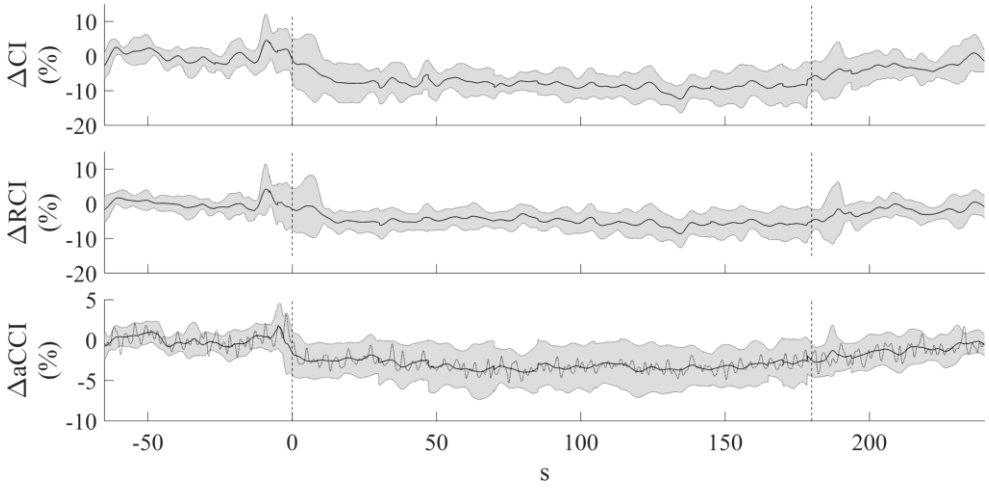

575

576 **Fig. 6.** Inferior Vena Cava collapsibility indexes averaged (across subjects) time course.
577 Absolute changes with respect to the mean baseline value of Caval Index (ΔCI), Respiratory
578 Caval Index (ΔRCI) and averaged Cardiac Caval Index (ΔaCCI): the black solid line represents
579 the mean while the shaded grey error bar represents mean ± std. The latter graph presents also
580 a superimposed dashed line trace that is the native Cardiac Caval Index: note the oscillations
581 due to the respiratory modulation of the cardiac induced pulsatility which are removed in the
582 aCCI trace (black solid line). The vertical dashed lines mark the beginning (left one) and the
583 end (right one) of the PLR.

584

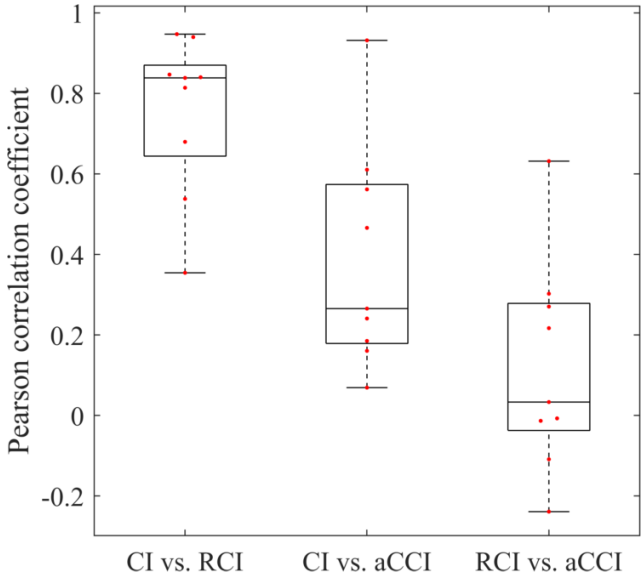

585

586 **Fig. 7.** Inferior vena cava collapsibility indexes correlations. Distributions of individual mutual

587 correlations among inferior vena cava collapsibility indexes, computed during baseline.

588

589 # Tables and Appendices

Variable	Baseline	PLR	DELTA %	p-value
Heart Rate (bpm)	59 ± 9	59 ± 10	0 ± 3	0.82
Mean Arterial Pressure (mmHg)	89 ± 11	90 ± 9	1 ± 6	0.43
Cardiac Output (L/min)	5.0 ± 0.8	5.1 ± 0.7	4 ± 4	0.03
Caval Index (%)	27 ± 6	19 ± 7	-31 ± 17	0.004
Respiratory Caval Index (%)	14 ± 4	9 ± 4	-35 ± 17	0.004
averaged Cardiac Caval Index (%)	13 ± 4	9 ± 4	-28 ± 21	0.008

590

591 **Table 1.** Averaged values of Heart Rate, Mean Arterial Pressure, Cardiac Output, Caval Index,
592 Respiratory Caval Index, and averaged Cardiac Caval Index in absolute values, during baseline
593 and PLR, and in terms of percentage variation during PLR w.r.t the mean baseline value
594 (DELTA). Values are expressed as MEAN ± STD. Last column reports the p-value of the
595 paired statistical comparison, by means of a paired Wilcoxon signed rank test, among the two
596 distributions of PLR and baseline individually averaged values.